

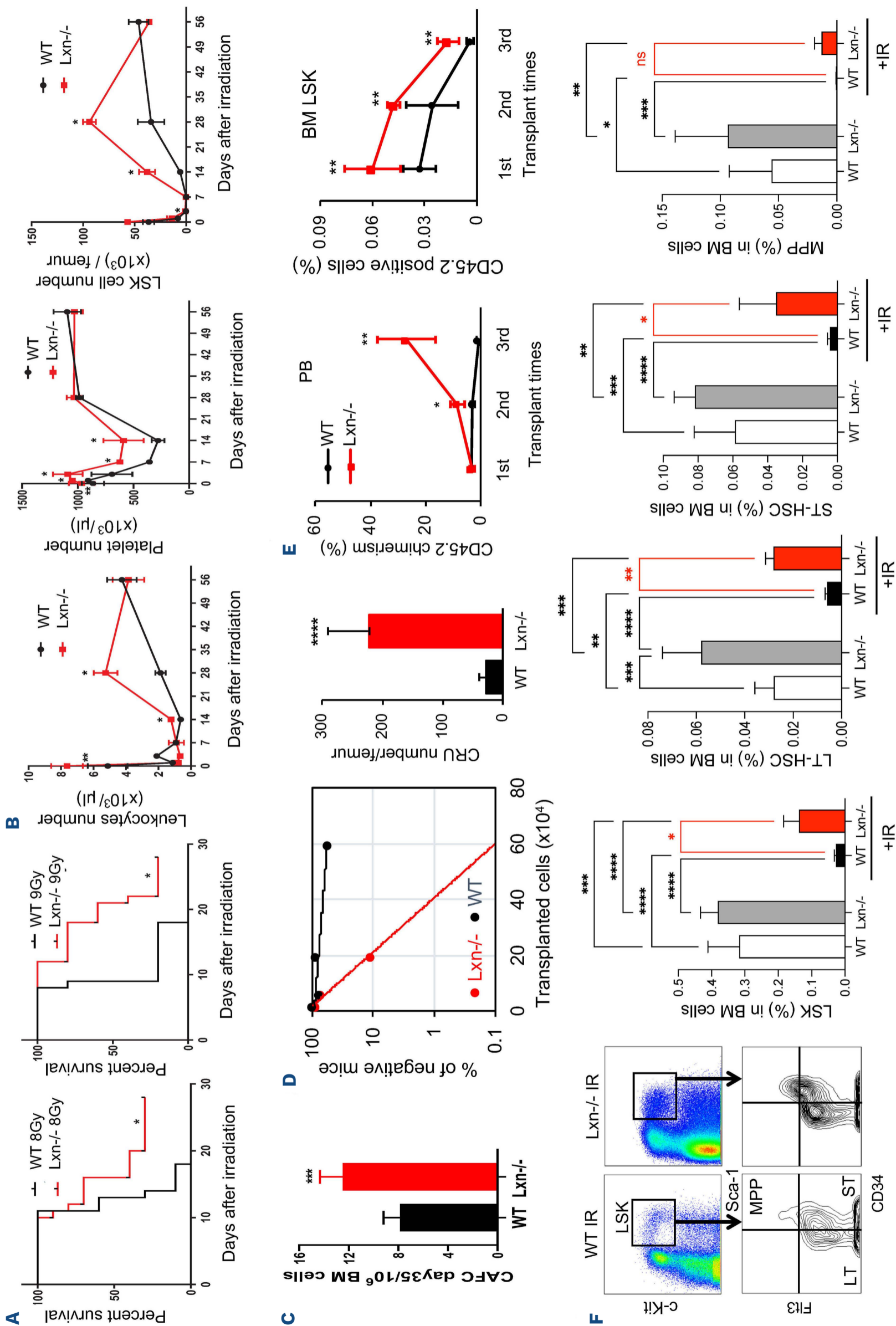
Latexin deletion protects against radiation-induced hematopoietic damages via selective activation of Bcl-2 prosurvival pathway

Exposure to ionizing radiation (IR) causes dysfunction of multiple organs of which the hematopoietic system is the most sensitive tissue.¹ Radiation damage to the hematopoietic system induces acute myelosuppression that increases the risk of infection and bleeding.² It also causes long-term bone marrow (BM) injury, which underlies the development of BM failure or hematological malignancies.³ Therefore, IR-induced acute and long-term BM injuries are the most significant consequence of accidental or intentional exposure to IR and also represent a serious side effect of radiation therapy.

To date, few effective medical countermeasures have been developed to protect and mitigate radiation-induced hematological toxicity. Recently, a significant progress has been made toward identifying novel radioprotectants, such as toll-like receptor 5 agonists⁴ and CDK4/6 inhibitors⁵, inhibitors of the protein C (aPC) pathway,⁶ and cell-based therapy such as infusion of endothelial or progenitor cells.⁷ However, further novel approaches, based on mechanistic data, are warranted since the translation of these findings into the clinic remains a significant challenge. Elucidating cellular and molecular pathways that govern the high sensitivity of hematopoietic cells, particularly hematopoietic stem cells (HSC), to IR can provide a better strategy to rationally develop medical countermeasures against radiation-induced hematopoietic toxicity.

We previously discovered that lack of the protein latexin (Lxn) in HSC enhances HSC survival and regeneration *in vivo*, while Lxn overexpression sensitizes myeloid cell line to radiation.^{8,9} In this study, we examined the role of Lxn in IR-induced BM injury and HSC damage using the Lxn knock-out mouse model (Lxn^{-/-}). Lxn^{-/-} mice have a significantly increased survival advantage compared to wild-type (WT) mice after lethal doses (8 Gy and 9 Gy) of total body irradiation (TBI) (Figure 1A). IR-induced acute myelosuppression is a primary cause of lethality. Therefore, we monitored the dynamic changes of blood and BM cells at different time points for 2 months post a sub-lethal dose (6.5 Gy) of TBI, and found that blood leukocytes and platelets and BM hematopoietic stem/progenitor cell (HSPC)-enriched lineage-Sca1⁺c-Kit⁺ (LSK) cells recovered significantly faster in Lxn^{-/-} mice than WT mice during the first month post-IR (Figure 1B). The rapid recovery was not due to the increased proliferation of LSK cells (*Online Supplementary Figure S1A*). We next determined the role of Lxn deletion in protecting HSC from radiation-induced long-

term damage. We irradiated Lxn^{-/-} and WT mice with 6.5 Gy TBI, collected BM cells at 56 days post-IR at which time blood cell and HSPC counts returned to the normal level (Figure 1B), and performed various functional assays to evaluate HSC regeneration and self-renewal functions, including cobblestone area forming cell (CAFC) assay, *in vivo* limiting dilution competitive repopulation unit (CRU) assay, and serial transplantation. The results showed that Lxn^{-/-} BM had a significantly elevated number of CAFC day 35 cells compared to the WT mice after IR (Figure 1C). The CRU assay showed that Lxn^{-/-} mice indeed preserved a significantly higher frequency of long-term repopulating HSC in the BM (Figure 1D). In competitive repopulation and serial transplantation, BM cells (CD45.2) from irradiated Lxn^{-/-} and WT mice were transplanted into lethally irradiated primary recipient mice (CD45.1) along with an identical number of competitor cells (CD45.1). At 16 weeks post-transplantation, PB and BM chimerism was analyzed for CD45.2-derived cells, and CD45.2 BM cells were sorted and transplanted into the secondary recipients. The same regimen was repeated in the tertiary transplantation. The result showed that Lxn^{-/-} HSC had a higher capacity to regenerate PB and BM LSK cells in the secondary and tertiary recipients than WT HSC (Figure 1E), demonstrating enhanced HSC self-renewal activity.¹⁰ Mice or humans exposed to radiation, especially fractionated low-dose radiation regimen, exhibit residual HSC functional defects even months after hematopoiesis has recovered from the exposure.¹¹ We exposed Lxn^{-/-} and WT mice with clinically relevant fractionated low-dose radiation (2 Gy daily for 5 days), and examined the long-term effect at a 16-20-month period post-IR along with age-matched non-IR WT and Lxn^{-/-} mice. We found that numbers of BM LSK cells, long-term (LT-), short-term HSC (ST-HSC), and multipotent progenitors (MPP), identified by flow cytometry, were much better preserved in Lxn^{-/-} mice compared to WT mice after radiation although radiation reduced the numbers of these cell populations in both strains (Figure 1F). Radiation induces the accumulation of reactive oxygen species (ROS) and senescence, and DNA damage. We didn't find any changes in ROS level and senescence in irradiated Lxn^{-/-} LSK cells compared to WT cells (*Online Supplementary Figure S1B, C*). By using γ -H2A.X staining and the comet assay, we found that Lxn^{-/-} LSK cells had fewer γ -H2A.X foci and a shorter length of comet tail post-IR compared to WT cells (*Online Supplementary Figure S1D, E*), suggest-



Continued on following page.

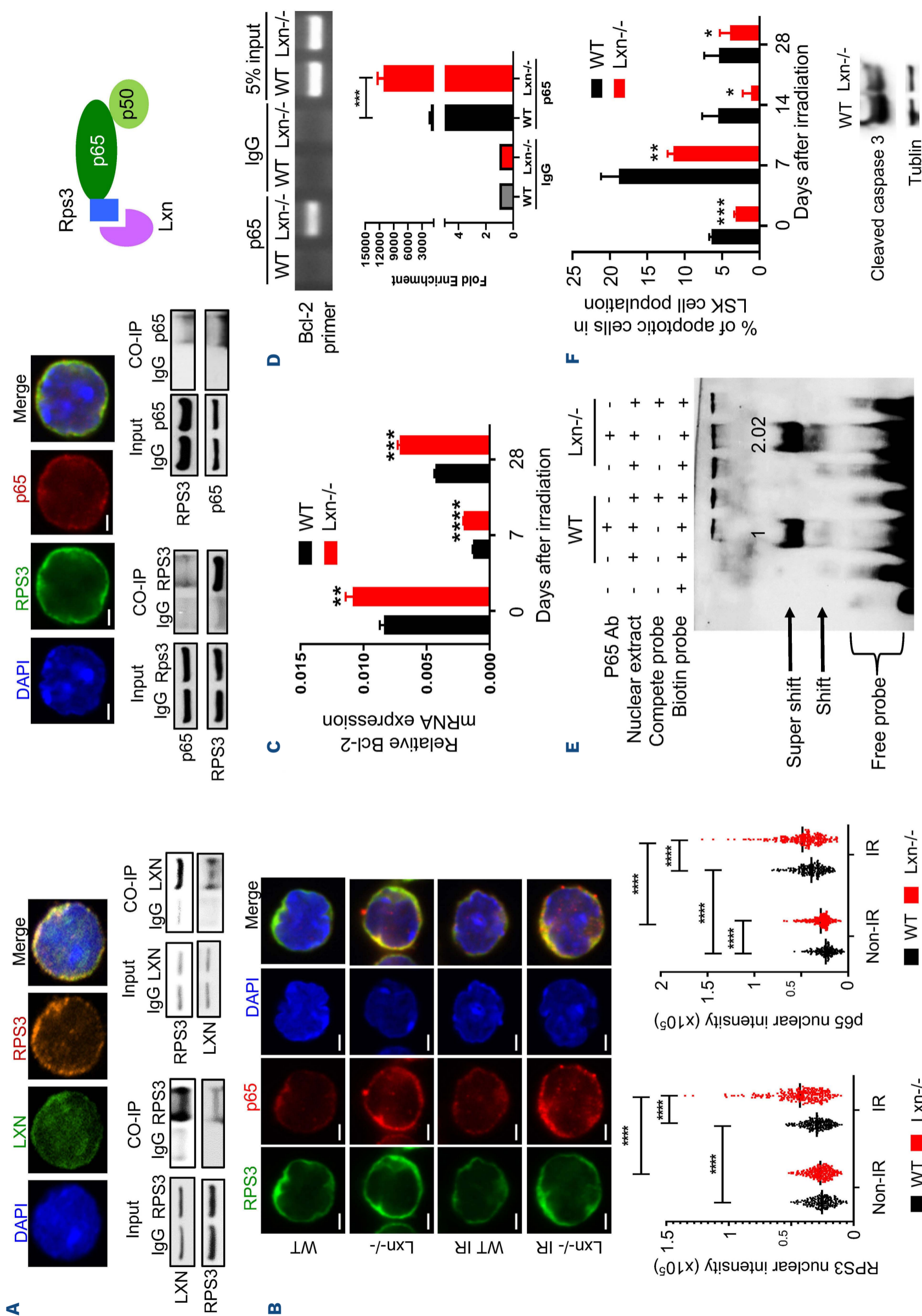
Figure 1. Latexin deletion protects radiation-induced acute myelosuppression and long-term hematopoietic stem cells functional impairment.

(A) Significant more latexin knock-out ($Lxn^{-/-}$) mice survived after exposure to 8 Gy (left) or 9 Gy (right) of total body irradiation (TBI) in 137 Cesium from JL Shepard Mark I irradiator. The mean survival time for $Lxn^{-/-}$ mice was 16 days compared to 13 days of wild-type (WT) mice in 8 Gy TBI. The mean survival time for $Lxn^{-/-}$ mice was 21 days compared to 9 days in 9 Gy TBI. Prism software was used to determine the mean survival time ($N=5$ /group). (B) $Lxn^{-/-}$ mice had accelerated recovery in the numbers of blood leukocytes, platelets, and hematopoietic stem/progenitor cells (HSPC) post sublethal 6.5 Gy TBI. HSPC was identified as Lin^{-} , $Sca1^{+}$, $c-kit^{+}$ cells (LSK cells). Data were collected on days 0, 1, 3, 7, 14, 28, and 56 days post-TBI ($N=5$ /group at each time point). (C-E) WT and $Lxn^{-/-}$ mice were subject to 6.5 Gy TBI. BM cells were isolated from these mice at 56 days post-TBI and evaluated for the HSC function by cobblestone area forming cell (CAFC) assay, limiting dilution competitive repopulation unit (CRU) assay, and competitive repopulation and serial transplantation. (C) More CAFC day 35 bone marrow (BM) cells were preserved in $Lxn^{-/-}$ mice after IR. BM cells were pooled from 5 mice in each group ($N=5$). Two independent CAFC assays were performed. (D) CRU frequency (left panel) and absolute number per femur (right panel) were significantly higher in $Lxn^{-/-}$ mice compared to WT mice. 2×10^4 , 6×10^4 , 2×10^5 or 6×10^5 donor BM cells were collected from $Lxn^{-/-}$ or WT (CD45.2) mice at day 56 after 6.5 Gy TBI, and mixed with 2×10^5 competitor BM cells (CD45.1) and retro-orbitally injected into lethally irradiated (9 Gy) recipient mice (CD45.1). Percentages of donor (CD45.2⁺)-derived peripheral blood (PB) cells were determined at 16 weeks post transplantation ($N=10$ recipient mice in each dilution). CRU frequency was calculated with LDA software. (E) In serial transplantation, $Lxn^{-/-}$ HSC had a higher capacity to regenerate PB and BM LSK cells in secondary and tertiary recipients. 1×10^6 donor cells from $Lxn^{-/-}$ or WT BM (CD45.2) mice were mixed with an equal number of competitor BM cells (CD45.1) and retro-orbitally injected into lethally irradiated (9 Gy) first recipient mice (CD45.1). At 16 weeks post-transplant, $Lxn^{-/-}$ or WT BM cells (CD45.2) were sorted from the primary recipients and transplanted into secondary recipients. An identical regimen was repeated one more time, culminating in the engrafted tertiary hosts. Percentages of CD45.2-derived PB and BM LSK cells were evaluated in each round of transplantation recipients ($N=10$ recipient mice at each time point). (F) Age-matched (8 weeks old) WT and $Lxn^{-/-}$ mice with or without the fractionated dose TBI (2 Gy daily for 5 days) were aged naturally for 16-20 months, and HSPC populations were analyzed for long-term effect. Representative flow cytometry analysis of HSPC subsets. Gating strategy for HSPC-enriched Lin^{-} , $Sca1^{+}$, $c-kit^{+}$ (LSK) cells, long-term HSC (LT-HSC) (LSK, CD34⁻, Flt3⁻), short-term HSC (ST-HSC) (LSK, CD34⁺, Flt3⁻), and multipotent progenitor (MPP) (LSK, CD34⁺, Flt3⁺) is shown. Percentages of LSK cells, LT-HSC, ST-HSC, and MPP cells were significantly higher in $Lxn^{-/-}$ mice than in WT mice ($N=5$ /group). The statistical analysis was consulted with the Markey Cancer Center Biostatistics & Bioinformatics Shared Resource Facility. Data were examined for homogeneity of variances (F test), then analyzed by a two-tailed, unpaired Student's *t* test. The log-rank (Mantel-Cox) test was used to assess survival curves. All statistical analyses were performed using GraphPad Prism Software version 7.0. Differences were considered significant at $P < 0.05$. Results shown represent mean \pm standard deviation; * $P \leq 0.05$, ** $P < 0.01$, *** $P < 0.001$ and **** $P < 0.0001$. Female mice were used at the age 7-8 weeks old. Mice were housed and handled at the University of Kentucky animal facilities following National Institutes of Health-mandated guidelines for animal welfare and with Institutional Animal Care and Use Committee approval number 2021-3881.

ing that survived $Lxn^{-/-}$ LSK cells maintained the genomic integrity. This may explain the absence of hematologic malignancies in $Lxn^{-/-}$ mice even 2 years after radiation (*data not shown*). Overall, all these short-term and long-term studies strongly suggest that *Lxn* deletion protects against both IR-induced acute myelosuppression and long-term HSC damage.

We determined the signaling pathways involved in *Lxn* deletion-mediated radiation protection. We previously identified ribosome protein subunit 3 (*Rps3*) as a novel *Lxn*-binding protein in a myeloid cell line.⁹ *Rps3* was reported to interact with the NF- κ B p65 subunit and direct the complex to the promoter of some specific pro-survival genes upon IR, thus providing regulatory specificity.^{12,13} We performed immunofluorescence staining in LSK cells and co-immunoprecipitation (Co-IP) in Lin^{-} cells, and confirmed the binding of *Lxn* and *Rps3*, and the interaction between *Rps3* and p65 in primary HSPC (Figure 2A). *Lxn* deletion didn't change *Rps3* mRNA level before and after radiation (*Online Supplementary Figure S2A*). *Rps3* itself is involved in ribosome assembly and protein synthesis. We asked whether *Lxn* deletion could affect protein synthesis in HSPC. We performed *in vivo* O-propargyl-puromycin (OP-Puro) incorporation assay and found similar OP-puro incorporation between different subsets of $Lxn^{-/-}$ and WT cells except for the CMP, indicating that *Lxn* deletion did

not affect overall protein synthesis in hematopoietic cells (*Online Supplementary Figure S2B*).¹⁴ We thus hypothesized that *Lxn* deletion releases *Rps3* protein, which promotes the nuclear translocation of the NF- κ B complex and stimulates prosurvival pathways upon radiation, enhancing HSC survival. We used immunofluorescence-conjugated *Rps3* and p65 antibodies to detect their signal intensity in the nucleus of single LSK cells and found there were more *Rps3* and NF- κ B p65 detected in the nucleus of $Lxn^{-/-}$ LSK cells compared with WT LSK cells post-IR (Figure 2B), suggesting that *Lxn* deletion does enhance nuclear translocation of the *Rps3*-NF- κ B complex. This result was further confirmed by western blot in less primitive Lin^{-} cells (*Online Supplementary Figure S2C*). We further identified *Bcl-2* as one of the downstream target survival genes that were upregulated in $Lxn^{-/-}$ LSK cells (Figure 2C; *Online Supplementary Figure S2D*). Chromatin immunoprecipitation quantitative polymerase chain reaction (ChIP-qPCR) and electrophoretic mobility shift assay (EMSA) confirmed that *Bcl-2* was the direct target of NF- κ B p65 in $Lxn^{-/-}$ cells, and there was more binding in $Lxn^{-/-}$ cells compared with WT cells (Figure 2D, E). Consistently, we found that $Lxn^{-/-}$ LSK cells were less apoptotic than WT cells at different time points after radiation (Figure 2F). All these data confirm that *Lxn* deletion promotes nuclear translocation of the *Rps3*-NF- κ B complex upon IR and activates *Bcl-2* tran-



Continued on following page.

Figure 2. Latexin deletion upregulates RPS3-NF- κ B-mediated transcriptional activation of Bcl-2 upon radiation and increases hematopoietic stem/progenitor cell survival. (A) Immunofluorescence staining shows the co-localization of LXN and RPS3, as well as RPS3 and NF- κ B p65 in a single LSK cell (top panel). Binding of LXN and RPS3, as well as RPS3 and NF- κ B p65 in Lin⁻ cells was confirmed by reciprocal co-immunoprecipitation (CO-IP, bottom panel). (B) Lxn^{-/-} LSK cells had increased nuclear translocation of RPS3 and NF- κ B p65 after ionizing radiation (IR). Representative microimages of RPS3 and p65 staining in single LSK cell from Lxn^{-/-} and wild-type (WT) mice with (6.5 Gy) or without IR (top panel). RPS3 (bottom left panel) and p65 (bottom right panel) staining intensity in the nuclear of LSK cells from Lxn^{-/-} and WT mice without or with IR (6.5 Gy) were quantified and presented (N=50-70 LSK cells evaluated per group). (C) Increased Bcl-2 mRNA expression of LSK cells from Lxn^{-/-} mice compared with WT mice at day 0, 7 and 28 after 6.5 Gy total body irradiation (TBI). Quantitative real-time polymerase chain reaction (PCR) was performed. mRNA was extracted from a pool of 5 mice/group. Two independent real-time PCR were performed and each experiment has 3 replicates. The data were pooled from 2 experiments. (D) Bcl-2 was a direct target of p65 and more p65 was enriched in the Bcl-2 promoter in Lxn^{-/-} Lin⁻ cells compared to WT cells. Chromatin immunoprecipitation assay was performed by p65 antibody and Bcl-2 promoter sequence was determined by real-time PCR. The gel image (top panel) and quantification (bottom panel) of real-time PCR were shown. (E) Electrophoresis mobility shift assay shows the direct binding of p65 to Bcl-2 promoter sequence, and more binding was present in Lxn^{-/-} Lin⁻ cells compared to WT cells at day 28 days post 6.5 Gy TBI. The quantification of the super shift band is labeled. (F) Percentage of apoptotic (Annexin V⁺ 7-AAD⁻) LSK cells was significantly lower in Lxn^{-/-} mice than WT mice at day 0, 7, 14, and 28 days post 6.5 Gy TBI (top panel), consistent with the decreased expression of cleaved caspase 3 in LSK cells at day 28 (bottom panel) (N=5 mice/group); *P< 0.05, **P<0.01, ***P<0.001, and ****P< 0.0001.

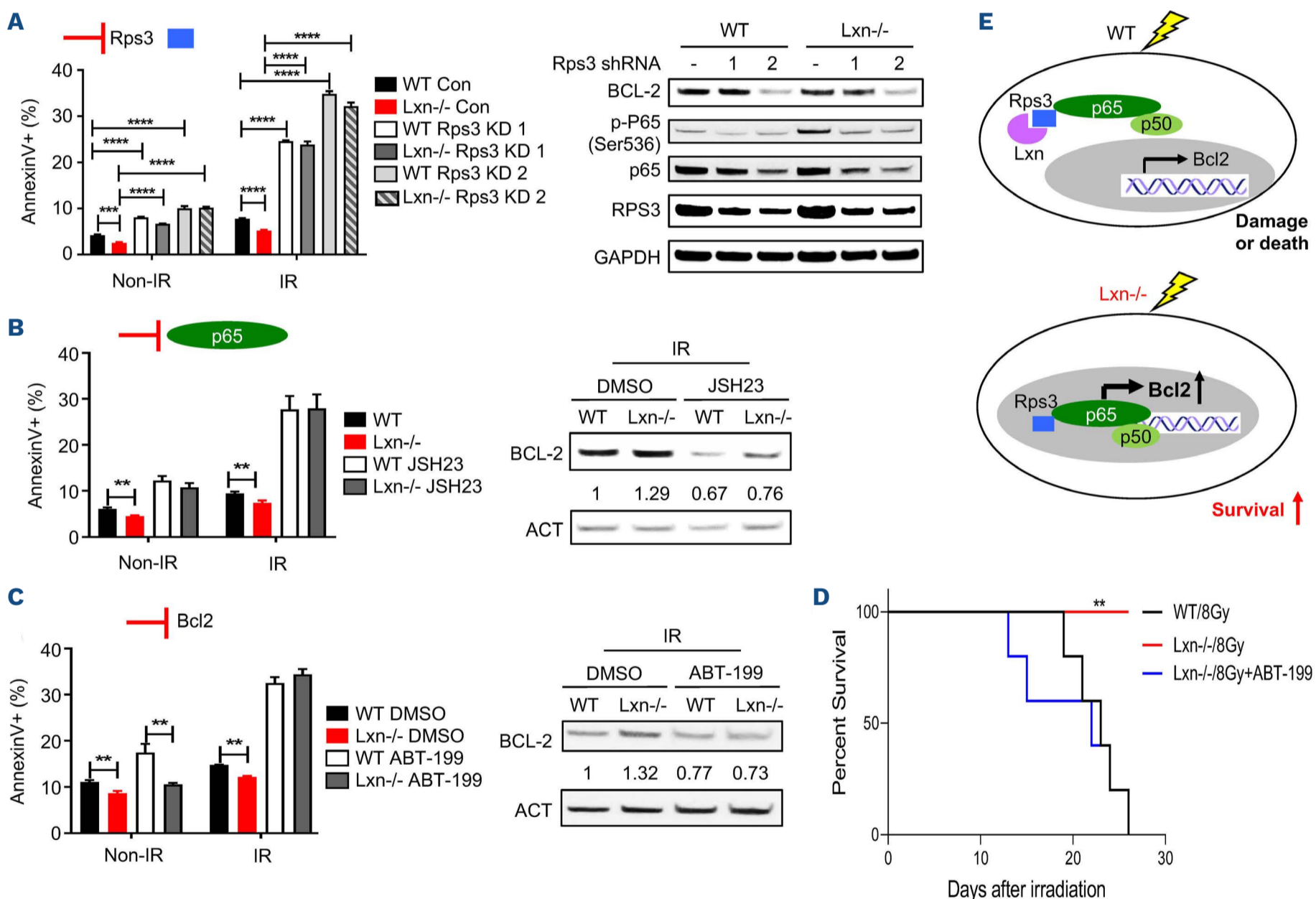


Figure 3. Inhibition of Rps3-NF κ B p65-Bcl-2 pathway sensitizes Lxn^{-/-} LSK cells to radiation-induced apoptosis. (A) Knock-down of Rps3 increases apoptosis of wild-type (WT) and Lxn^{-/-} LSK cells and diminishes their survival difference without or with ionizing radiation (IR) (left panel). Consistently, knockdown of Rps3 decreased p65, phosphorylated p65 (p-p65), and Bcl-2 expression (right panel). Flow cytometry-sorted LSK cells from WT or Lxn^{-/-} mice were stimulated with cytokines including 100 ng/mL FMS-like tyrosine kinase-3 ligand, 50 ng/mL mouse stem cell factor, 20 ng/mL interleukin-3 (IL-3), and 20 ng/mL TPO in StemSpan SFEM (STEMCELL Technologies). After 24 hours (hrs), the cells were transduced with lentiviral particles encoding Rps3 small hairpin RNA (shRNA) (catalog no: MSH030789-LVRU6GP, GeneCopoeia) or its related scramble control vector, at a MOI of 100 along with 8 μ g/mL polybrene for 6 hrs at 37°C. After 48 hrs, the GFP-positive cells were sorted for apoptosis assay and western blot. (B) NF- κ B p65 specific inhibitor, JSH23, leads to the increased apoptosis of WT and Lxn^{-/-} LSK cells and diminishes their apoptosis difference without or with IR (left panel). JSH23 also results in decreased Bcl-2 expression in both WT and Lxn^{-/-} LSK

Continued on following page.

cells (right panel). The fold change of each protein expression was marked underneath. (C) Bcl-2 specific inhibitor, ABT-199, leads to the increased apoptosis of WT and *Lxn*^{-/-} LSK cells and diminishes their apoptosis difference without or with IR (left panel). It also inhibits Bcl-2 expression in *Lxn*^{-/-} LSK cells (right panel). The fold change of each protein expression was marked underneath. In (B and C), sorted WT or *Lxn*^{-/-} LSK cells were cultured in StemSpan SFEM (STEMCELL Technologies) with cytokines including 100 ng/mL FMS-like tyrosine kinase-3 ligand, 50 ng/mL mouse stem cell factor, 20 ng/mL interleukin-3 (IL-3), and 20 ng/mL TPO. Immediately after 6.5 Gy irradiation, P65 inhibitor II, JSH23 (final concentration 7.1 μm, Millipore Sigma, catalog# 481408), or Bcl-2 inhibitor, ABT-199 (final concentration 100 μm, CHEMIETEK, catalog# CT-A199) or control (dimethyl sulfoxide [DMSO]), was added into the cells. After 6 hrs, cells were collected for apoptosis analysis or western blot. Apoptosis was measured by Annexin V⁺ 7AAD. Protein expression was measured by western blot. Two independent experiments were performed and each experiment has 3 replicates; ***P*<0.01, ****P*<0.001, *****P*<0.0001. (D) *In vivo* treatment of *Lxn*^{-/-} mice by ABT-199 suppresses the survival advantage of radiation. New cohorts of WT and two groups of *Lxn*^{-/-} mice were subject to 8 Gy TBI. One group of *Lxn*^{-/-} mice was intraperitoneally injected with ABT-199 the day after total body irradiation (TBI) with a dose 100 mg/kg daily for 1 week. Mice survival was monitored and the mean survival time was calculated by using Prism software. The mean survival times for WT group and *Lxn*^{-/-} group with ABT-199 post TBI were 23 days and 22 days respectively, whereas *Lxn*^{-/-} group all survived during the 30 days of observation. The mice used in this experiment were 16–18 weeks old females (N=5/group); ***P*<0.01. (E) Model of the molecular mechanism for *Lxn* deletion-mediated radiation protection. *Lxn* binds to Rps3. Rps3 is an integral component of the NF-κB complex (p65/p50 dimer) by its specific interaction with the p65 subunit. In the absence of *Lxn*, Rps3 enhances the nuclear translocation of the NF-κB complex upon radiation and guides NF-κB complex specifically binding to the promoter of the prosurvival gene, Bcl-2, and increases its transcription and expression. This leads to the increased survival of *Lxn*^{-/-} hematopoietic stem/progenitor cells upon radiation.

scription, thus enhancing the survival of *Lxn*^{-/-} HSPC. We next genetically or pharmaceutically inhibited each key component of the Rps3- NF-κB-Bcl-2 pathway in *Lxn*^{-/-} LSK cells and determined whether it could blunt the survival advantage upon radiation. Annexin V⁺ apoptotic cells and Bcl-2 expression were used for functional and molecular evaluation. Rps3 knock-down increased apoptosis in both WT and *Lxn*^{-/-} cells, abolished the survival advantage of *Lxn*^{-/-} cells, and suppressed both NF-κB p65 nuclear translocation and Bcl-2 expression (Figure 3A). We next treated cells with the NF-κB specific inhibitor JSH-23 and found that NF-κB inhibition also attenuated radiation protection and Bcl-2 activation in *Lxn*^{-/-} cells (Figure 3B). Similar effects were observed with the Bcl-2 specific inhibitor ABT-199 (Figure 3C). In order to further confirm the relationship between *Lxn* and Bcl2 *in vivo*, we treated *Lxn*^{-/-} mice with ABT-199 *in vivo* after lethal IR (8 Gy), and found that ABT-199 diminished the survival advantage of *Lxn*^{-/-} mice after IR in comparison to the irradiated WT and *Lxn*^{-/-} mice without treatment (Figure 3D). Altogether, these data suggest that in the absence of *Lxn*, HSC are protected from radiation-induced apoptosis via activation of a novel Rps3-NF-κB-Bcl-2 prosurvival pathway (Figure 3E). *Lxn* has thus a unique dual function in that it provides protection against both acute and long-term hematopoietic damages upon radiation. *Lxn* is a novel regulator of NF-κB signaling pathway via the specific interaction to Rps3 protein. Such Rps3-dependent activation of specific NF-κB target genes has been proposed as a novel strategy to selectively, rather than globally, manipulate NF-κB activity to reduce off-target side effects.^{12,13,15} In the future, an investigation of how *Lxn* is involved in this pathway will be warranted. *Lxn* might be a new target for developing novel radiomitigation compounds to minimize radiation-induced injury. Moreover, we have reported that *Lxn*^{-/-} mice had better hematopoietic recovery from 5-FU-induced myelo-

suppression.⁸ Pharmacological inhibition of *Lxn* could be of clinical importance in improving outcomes for patients with radiation and chemotherapy.

Authors

Cuiping Zhang,¹ Xiaojing Cui,¹ Yi Liu,² Fang Wang,¹ Robert Signer,³ Kapana Nattamai,⁴ Daohong Zhou,⁵ Yi Zheng,⁴ Hartmut Geiger,⁶ Fengyi Wan⁷ and Ying Liang^{6*}

¹Department of Toxicology and Cancer Biology University of Kentucky, Lexington, KY, USA; ²Department of Physiology, University of Kentucky, Lexington, KY, USA; ³Division of Regenerative Medicine, Department of Medicine, Moores Cancer Center, University of California San Diego, La Jolla, CA, USA; ⁴Experimental Hematology and Cancer Biology, Cincinnati Children Hospital Medical Center, University of Cincinnati, OH, USA; ⁵Department of Biochemistry & Structural Biology, University of Texas Health Science Center, San Antonio, TX, USA; ⁶Institute of Molecular Medicine, Ulm University, Ulm, Germany and ⁷Department of Biochemistry and Molecular Biology, Bloomberg School of Public Health, Johns Hopkins University, Baltimore, MD, USA

*current address: New York Blood Center, New York, NY, USA

Correspondence:

Y. LIANG - yliang@nybc.org

<https://doi.org/10.3324/haematol.2022.282028>

Received: September 8, 2022.

Accepted: June 15, 2023.

Early view: June 22, 2023.

©2023 Ferrata Storti Foundation

Disclosures

The work is related to a patent US 10,604,756.

Contributions

CZ performed the majority of experiments and wrote the manuscript. XC was involved in Lxn^{-/-} mice maintenance. YLiu helped with blood and bone marrow cell monitoring. FW did the ABT-199 survival experiment. RS helped with protein synthesis and review of the manuscript. DZ, YZ, KN, FW, and HG helped with the radiation strategy and phenotype characterization, and manuscript revision. YLiang guided the overall project, designed the experiments, and wrote the manuscript.

Acknowledgments

We thank the Markey Cancer Center's Research Communications

Office for editing and graphics support. We thank Dr. Sean Morrison for the critical insights into studies and comments on manuscripts.

Funding

The authors are supported by the National Institutes of Health under awards R01HL124015(YL), R21HL140213 (to YL), R43AI145726 (to YL), and R01CA211963 (to DZ) and the Markey Cancer Center's Flow Cytometry and Immune Monitoring Core and Biostatistics and Bioinformatics Shared Resource Facilities (P30CA177558).

Data-sharing statement

All data generated or analyzed during this study are included in this published article (and its *Online Supplementary Appendix*). Data will be available from the corresponding author upon reasonable request.

References

1. Mauch P, Constone L, Greenberger J, et al. Hematopoietic stem cell compartment: acute and late effects of radiation therapy and chemotherapy. *Int J Radiat Oncol Biol Phys*. 1995;31(5):1319-1339.
2. Shao L, Luo Y, Zhou D. Hematopoietic stem cell injury induced by ionizing radiation. *Antioxid Redox Signal*. 2014;20(9):1447-1462.
3. Harbron RW, Feltbower RG, Glaser A, Lilley J, Pearce MS. Secondary malignant neoplasms following radiotherapy for primary cancer in children and young adults. *Pediatr Hematol Oncol*. 2014;31(3):259-267.
4. Burdelya LG, Krivokrysenko VI, Tallant TC, et al. An agonist of toll-like receptor 5 has radioprotective activity in mouse and primate models. *Science*. 2008;320(5873):226-230.
5. Johnson SM, Torrice CD, Bell JF, et al. Mitigation of hematologic radiation toxicity in mice through pharmacological quiescence induced by CDK4/6 inhibition. *J Clin Invest*. 2010;120(7):2528-2536.
6. Geiger H, Pawar SA, Kerschen EJ, et al. Pharmacological targeting of the thrombomodulin-activated protein C pathway mitigates radiation toxicity. *Nat Med*. 2012;18(7):1123-1129.
7. Chute JP, Muramoto GG, Salter AB, et al. Transplantation of vascular endothelial cells mediates the hematopoietic recovery and survival of lethally irradiated mice. *Blood*. 2007;109(6):2365-2372.
8. Liu Y, Zhang C, Li Z, et al. Latexin Inactivation Enhances survival and long-term engraftment of hematopoietic stem cells and expands the entire hematopoietic system in mice. *Stem Cell Rep*. 2017;8(4):991-1004.
9. You Y, Wen R, Pathak R, et al. Latexin sensitizes leukemogenic cells to gamma-irradiation-induced cell-cycle arrest and cell death through Rps3 pathway. *Cell Death Dis*. 2014;5(10):e1493.
10. Liang Y, Jansen M, Aronow B, Geiger H, Van Zant G. The quantitative trait gene latexin influences the size of the hematopoietic stem cell population in mice. *Nat Genet*. 2007;39(2):178-188.
11. Chua HL, Plett PA, Fisher A, et al. Lifelong residual bone marrow damage in murine survivors of the hematopoietic acute radiation syndrome (H-ARS): a compilation of studies comprising the Indiana University Experience. *Health Phys*. 2019;116(4):546-557.
12. Wan F, Anderson DE, Barnitz RA, et al. Ribosomal protein S3: a KH domain subunit in NF-kappaB complexes that mediates selective gene regulation. *Cell*. 2007;131(5):927-939.
13. Wan F, Weaver A, Gao X, et al. IKKbeta phosphorylation regulates RPS3 nuclear translocation and NF-kappaB function during infection with Escherichia coli strain O157:H7. *Nat Immunol*. 2011;12(4):335-343.
14. Signer RA, Magee JA, Salic A, Morrison SJ. Haematopoietic stem cells require a highly regulated protein synthesis rate. *Nature*. 2014;509(7498):49-54.
15. Wier EM, Neighoff J, Sun X, Fu K, Wan F. Identification of an N-terminal truncation of the NF-kappaB p65 subunit that specifically modulates ribosomal protein S3-dependent NF-kappaB gene expression. *J Biol Chem*. 2012;287(51):43019-43029.